Regularization Methods in Non-Rigid Registration :II. Isotropic Energies, Filters and Splines

Pascal Cachier, Nicholas Ayache

INRIA

INSTITUT NATIONAL DE RECHERCHE EN INFORMATIQUE ET EN AUTOMATIQUE

Regularization Methods in Non-Rigid Registration: II. Isotropic Energies, Filters and Splines.

Pascal Cachier, Nicholas Ayache

N° 4243

Août 2001

THÈME 3

ISSN 0249-6399 ISRN INRIA/RR--4243--FR+ENG

INRIA
SOPHIA ANTIPOLIS

Regularization Methods in Non-Rigid Registration: II. Isotropic Energies, Filters and Splines.

Pascal Cachier, Nicholas Ayache

Thème 3 — Interaction homme-machine,
images, données, connaissances
Projet Epidaure

Rapport de recherche n° 4243 — Août 2001 — 28 pages

Abstract:

The goal of this report is to propose some new regularization and filtering techniques specific to vector fields.

Indeed, most of vectorial regularization energies used in the domain of image or feature matching are in fact scalar energies applied independently on each component of the transformation. The only common exception is the elastic energy, which enables cross-effects between components.

In this report, we first propose a technique to find all isotropic differential quadratic forms (IDQF) of any order on vector fields, and give results in the case of order 1 and 2. The dense quadratic approximation induced by these energies give birth to a new class of vector filters, which are applied in practice in the Fourier domain. We also propose a family of isotropic and separable vector filters that generalize scalar Gaussian filtering to vectors and enables efficient isotropic smoothing without using Fourier transform, using recursive filtering in the real domain.

We also study the splines induced by these energies in the context of spare point motion interpolation or approximation. These splines are generalization to vectors of the scalar Laplacian splines, such as the thin-plate spline.

We finally propose to merge dense and sparse approximation problems, yielding solutions that mix convolution filter and splines. This enables to introduce naturally sparse geometric constraints into an intensity-based registration algorithm.

Key-words: Non-rigid registration, isotropy, differential quadratic forms, vector filters, Fourier transform, separable filters.

Unité de recherche INRIA Sophia Antipolis
2004, route des Lucioles, BP 93, 06902 Sophia Antipolis Cedex (France)
Téléphone : +33 4 92 38 77 77 — Télécopie : +33 4 92 38 77 65

Méthodes de régularisation en recalage non rigide d'images: II. Energies, filtres et splines isotropiques.

Résumé :

Le but de ce rapport de recherche est de proposer quelques techniques nouvelles de régularisation et de lissage spécifiques aux champs de vecteurs.

En effet, la plupart des énergies de régularisation vectorielle utilisées dans le domaine du recalage d'images ou d'amers sont en fait des énergies scalaires portant indépendamment sur chacune des composantes de la transformation. La seule exception fréquente est l'énergie élastique linéaire, qui autorise des effets croisés entre les composantes du champs de déplacements.

Dans ce rapport, nous proposons une technique permettant de trouver toutes les formes quadratiques différentielles isotropiques de tout ordre portant sur un champ de vecteur, et nous donnons les resultats dans le cas des ordres 1 et 2. L'approximation quadratique induite par ces énergies donne naissance à une nouvelle classe de filtres vectoriels, que nous appliquons numériquement dans le domaine de Fourier. Nous proposons également une famille de filtres isotropiques séparables qui généralise le lissage gaussien aux champs de vecteurs, et qui permet un lissage isotropique rapide sans utiliser de transformée de Fourier, en utilisant des filtres récursifs dans le domaine réel.

Nous étudions également les splines associées à ces énergies dans le contexte de l'interpolation ou de l'approximation du mouvement de points éparts. Ces splines sont une généralisation aux vecteurs des splines laplaciennes scalaires, comme les splines dites de plaque mince.

Nous proposons enfin de réunir les problèmes d'approximations dense et éparse. La solution explicite à ce problème s'avère être un mélange de lissage et d'approximation par splines. Cette dernière problematique permet d'introduire de manière élégante des contraintes géométriques dans des algorithmes de recalage non rigide iconiques.

Mots-clés : Recalage non rigide, isotropie, formes quadratiques différentielles, filtres vectoriels, transformée de Fourier, filtres séparables.

Contents

1 Introduction

This report focuses on smoothness energies of vectors fields based on their partial derivatives, such as the linear elastic or thin-plate energies.

In intensity-based non-rigid registration, the similarity energy alone is not sufficient to obtain a good estimate of the underlying transformation between two images, because it does not ensure any spatial coherence between the motion of two close points. The estimate of the motion has to be regularized, even if occasional discontinuities may be allowed in the deformation field (Hellier et al., 1999; Alvarez et al., 2000). Competitive algorithms (Cachier and Ayache, 2001) ensure this smoothness using a regularization energy that is minimized together with the similarity energy.

On one hand, many similarity measures have been studied. Let us just mention the recently introduced mutual information (Collignon et al., 1995; Wells et al., 1996), normalized mutual information (Studholme et al., 1999) and correlation ratio (Roche et al., 1998). Also, they have been compared in the case of rigid registration in many articles (Studholme et al., 1995; Roche et al., 1998; Nikou et al., 1999; Weese et al., 1999; Holden et al., 2000).

On the other hand, regularization energies of vector fields have been less focused on, and comparisons are quite rare. The only commonly used vectorial regularization used in non-rigid registration enabling cross-effects between the components of the vector field is the linear elastic energy (Miller et al., 1993; Gee et al., 1995; Ferrant et al., 1999). The other standard energies, such as the thin-plate (or bending) energy (Rueckert et al., 1999; Amini et al., 1999), are in fact regularization of scalar fields, applied independently on each component of the vector field.

In this report, we propose to study truly vectorial regularization energies, and more particularly differential quadratic forms (DQF). DQF are very often used as is for regularization (e.g., linear elasticity, thin plate energy, Gaussian filtering), but it is worth noting that even complex regularization energies are generally based on the same small set of differential quadratic form (DQF). The elastic or thin-plate DQF can be symmetrized (Cachier and Pennec, 2000), rewritten in an anisotropic way (Alvarez et al., 2000), inserted in a Mumford-Shah formulation (Tsai et al., 2000), non-uniformly weighted (Terzopoulos, 1986) or rewritten with M-estimators (Hellier et al., 1999), to obtain discontinuities — but all these energies starts from the same classical set of DQF.

This set of suitable DQF is restricted, because they should remain invariant by rotation and symmetry; in other words, they should be isotropic. In this report, we aim at finding the elements of this set, and the convolution filter and spline associated to these energies.

In section 2, we propose a technique to find all possible isotropic differential quadratic forms (IDQF) of vector fields, and apply it to IDQF of order 1 and 2.

In section 3, we deduce vector convolution filters from the previous IDQF. Contrary to conventional scalar filters which are applied independently on each component of the vector field, these vector filters allow cross-effects between its components, yielding more realistic motion.

In section 4, we deduce the splines associated with these IDQF, which are used for landmark point based registration. Again, contrary to conventional scalar splines (or radial basis functions) that are applied independently to each component, these vectorial splines allow cross-effects between the components; also, they are no more radial.

Finally, we merge dense and sparse vector approximation problems into the same energy, yielding a solution that is a linear combination of convolution and splines. This last formula-

tion is very useful to introduce landmark point constraints in an intensity-based registration algorithm.

2 Isotropic Differential Quadratic Forms

The goal of this section is to find all differential quadratic forms remaining invariant by rotation and symmetry. We show that a general theorem on isotropic tensors gives an explicit set of generators of isotropic DQF. Because DQF are tensors with specific symmetries, this set can be reduced, which is done in the case of isotropic DQF of order 1 and 2.

2.1 Some Mathematical Definitions

We note $\mathcal{M}(d)$ the group of linear functions of $\mathbb{R}^d$ in itself, and $O(d) \in \mathcal{M}(d)$ the orthogonal group composed of orthogonal linear functions R, such that $R^T.R = R.R^T = \mathrm{Id}_d$. Also, to avoid long mathematical expressions, we use in the following a (simplified version of)[1] Einstein summation convention, for which every index repeated twice in a product is implicitly summed all over its range. For example, if $\partial_i f, i \in \{x, y\}$ are the partial derivatives of a two-dimensional function f, then using Einstein convention,

$$\partial_i f \partial_i f \triangleq \sum_{i \in \{x,y\}} \partial_i f \partial_i f = (\partial_x f)^2 + (\partial_y f)^2$$

Definition 1 (Tensor) *A tensor T of order $n \geq 1$ in a space of dimension $d \geq 1$ is represented by d^n numbers, noted $T_{i_1 i_2 \ldots i_n}$, $i_j \in [\![1; d]\!]$, $\forall j \in [\![1; n]\!]$, which transform under the action of $A = (a_{ij}) \in \mathcal{M}(d)$ in the following way: if $A \star T$ is the resulting tensor, then*

$$A \star T_{i_1 \ldots i_n} = a_{i_1 j_1} \ldots a_{i_n j_n} T_{j_1 \ldots j_n}$$

We note $\mathcal{T}(n, d)$ the set of these tensors.

Definition 2 (Differential Tensor) *The partial derivatives $\partial_{i_1 \ldots i_n} f_{i_{n+1}}$ of a vector field $\mathbf{f}$ of dimension d form a tensor of $\mathcal{T}(n+1, d)$ called the n-th order differential tensor of $\mathbf{f}$.*

Definition 3 (Quadratic forms of tensors) *We note $\mathcal{Q}(n, d)$ the set of quadratic form of tensors $T \in \mathcal{T}(n, d)$, which can be represented by d^{2n} numbers $q_{i_1 \ldots i_n j_1 \ldots j_n}$, $(i_k, j_k) \in [\![1; d]\!]^2$, $\forall k \in [\![1; n]\!]$, so that*

$$q(T) = q_{i_1 \ldots i_n j_1 \ldots j_n} T_{i_1 \ldots i_n} T_{j_1 \ldots j_n}$$

with $q_{i_1 \ldots i_n j_1 \ldots j_n} = q_{j_1 \ldots j_n i_1 \ldots i_n}$.

Property 1 *If $q \in \mathcal{Q}(n, d)$, $T \in \mathcal{T}(n, d)$ and $A \in \mathcal{M}(d)$,*

$$A^T \star q(T) \triangleq q(A \star T) = q_{i_1 \ldots i_n j_1 \ldots j_n} a_{i_1 k_1} \ldots a_{i_n k_n} a_{j_1 l_1} \ldots a_{j_n l_n} a_{i_1 \ldots i_n j_1 \ldots j_n} T_{k_1 \ldots k_n} T_{l_1 \ldots l_n}$$

This last formula shows that the $q_{i_1 \ldots i_n j_1 \ldots j_n}$ form a tensor of order $2n$.

[1] Here, we do not need to distinguish between covariant and contravariant coordinates.

2.2 Isotropy

Definition 4 (Isotropic tensors) *A tensor $T \in \mathcal{T}(n,d)$ is isotropic if it is invariant by an orthogonal change of the tensor, i.e. if for any orthogonal function $R = (R_{ij}) \in O(d)$,*

$$R \star T = T$$

or, using prop. 1,

$$T_{i_1 \ldots i_n} = r_{i_1 j_1} \ldots r_{i_n j_n} T_{j_1 \ldots j_n} \quad \forall (i_1 \ldots i_n) \in [\![1; d]\!]^n$$

Definition 5 *Isotropic quadratic forms of the n-th order differential tensor of a vector field are called isotropic differential quadratic forms (IDQF). Its coefficients form an isotropic tensor of order $2n+2$.*

Theorem 1 *An isotropic tensor of order n, n even, can be written as a linear combination of the $n!/(2^{n/2}(n/2)!)$ products of Kronecker tensors $\delta_{i_r i_s}$. The only isotropic tensor of order n, n odd, is the null tensor.*

The demonstration of this result can be found in (Weyl, 1966; Jeffreys, 1973). This result can be applied to quadratic forms to give us a set of generators of IDQF. In the following we study the case of IDQF of order 1 and 2.

2.3 First-Order IDQF

According to Theorem 1, an isotropic tensor of order 4 is a linear combination of the three following tensors:

$$\delta_{i_1 i_2}\delta_{i_3 i_4} \quad \delta_{i_1 i_3}\delta_{i_2 i_4} \quad \delta_{i_1 i_4}\delta_{i_2 i_3}$$

Therefore, a first-order IDQF q, which can be regarded as a tensor of order 4 (Prop. 1), is a linear combination of the tensors $\partial_i f_i \partial_j f_j$, $\partial_i f_j \partial_i f_j$ and $\partial_i f_j \partial_j f_i$.

For any IDQF q of the first derivative of a vector field $\mathbf{f}$, we can find three coefficients a_1, a_2, a_3 so that

$$q(\mathbf{f}) = a_1.\mathrm{tr}(\nabla \mathbf{f}^T \nabla \mathbf{f}) + a_2.\mathrm{tr}(\nabla \mathbf{f} \nabla \mathbf{f}) + a_3.\mathrm{tr}(\nabla \mathbf{f})^2 \tag{1}$$

with

$$\begin{aligned} \mathrm{tr}(\nabla \mathbf{f}^T \nabla \mathbf{f}) &= \partial_i f_j \partial_i f_j \\ \mathrm{tr}(\nabla \mathbf{f} \nabla \mathbf{f}) &= \partial_i f_j \partial_j f_i \\ \mathrm{tr}(\nabla \mathbf{f})^2 &= \partial_i f_i \partial_j f_j \end{aligned} \tag{2}$$

2.4 Positive First-Order IDQF

A quadratic differential regularization energy should always be positive, in order to penalize high values of partial derivatives. Therefore, we should study the conditions on a_1, a_2 and a_3 for which the IDQF remains positive for every vector field $\mathbf{f}$.

To find out if a first-order IDQF is positive, we must find its eigenvalues. If all of them are positive, then the quadratic form is positive.

The linear function $Q : \mathcal{M}_n \to \mathcal{M}_n$ associated to q given by Equ. (1) is defined by:

$$Q(M) = a_1.M_{i,j}.E^{(i,j)} + a_2.M_{i,j}.E^{(j,i)} + a_3.M_{i,i}.E^{(j,j)}$$

where $E^{(i,j)}$ is the matrix of $\mathcal{M}_n$ whose only non-zero element is $E^{(i,j)}_{i,j} = 1$. It can be verified that the following matrices are eigenmatrices of Q:

Eigenmatrix	Eigenvalue
Id	$a_1 + a_2 + d.a_3$
$E^{(i,j)} + E^{(j,i)}, (i,j) \in [\![1;d]\!]^2, i \neq j$	$a_1 + a_2$
$E^{(i,j)} - E^{(j,i)}, (i,j) \in [\![1;d]\!]^2, i \neq j$	$a_1 - a_2$
$F_i, i \in [\![2;d]\!]$	$a_1 + a_2$

where $F_1 = \mathrm{Id}$ and $(F_1, ..., F_d)$ is an orthogonal basis of the space generated by the set $\{E^{(i,i)}, i \in [\![1;d]\!]\}$. Furthermore, all these eigenmatrices are orthogonal, and we have exactly $1 + d(d-1)/2 + d(d-1)/2 + (d-1) = d^2$ of them, so there does not exist any other eigenvalue than the three listed above.

Therefore, a first-order IDQF q is positive if we simultaneously have

$$\begin{aligned} a_1 + a_2 &\geq 0 \\ a_1 - a_2 &\geq 0 \\ a_1 + a_2 + d.a_3 &\geq 0 \end{aligned}$$

2.5 Second-Order IDQF

According to Theorem 1, an isotropic tensor of order 6 is a linear combination of products of Kronecker tensors of the form $\delta_{i_r i_s}\delta_{i_t i_u}\delta_{i_v i_w}$. There are 15 such tensors.

However, in the case of second-order IDQF, this set of generators can be reduced. First, it is known that the isotropic tensors given by Theorem 1 are not independent of each other. A minimal, independent set of isotropic tensors that generates all isotropic tensors by linear combination can be found for example in (Smith, 1968). Second, the quadratic forms we are interested in are tensors with specific symmetries, due to the commutation of multiplication and differentiation assumed here: this also reduces the number of functions necessary to generate second-order isotropic quadratic energies.

We can therefore eliminate some of the tensors given by theorem 1, based on the commutation of the multiplication and the differentiation. This is done in appendix A, and leads to the following result:

For any second-order IDQF of a vector field $\mathbf{f}$, we can find five coefficients a_1, a_2, a_3, a_4, a_5 so that

$$q(\mathbf{f}) = a_1.Q_1(\mathbf{f}) + a_2.Q_2(\mathbf{f}) + a_3.Q_3(\mathbf{f}) + a_4.Q_4(\mathbf{f}) + a_5.Q_5(\mathbf{f})$$

with

$$\begin{aligned} Q_1(\mathbf{f}) &= \partial_{ij} f_k \partial_{ij} f_k \\ Q_2(\mathbf{f}) &= \partial_{ij} f_j \partial_{ik} f_k \\ Q_3(\mathbf{f}) &= \partial_{ii} f_j \partial_{kk} f_j \\ Q_4(\mathbf{f}) &= \partial_{ij} f_k \partial_{kj} f_i \\ Q_5(\mathbf{f}) &= \partial_{ii} f_j \partial_{kj} f_k \end{aligned}$$

3 Isotropic Convolution Filters for Vector Fields

This section focuses on convolution filters for vector fields. We first start from the problem of quadratic approximation using the IDQF developed in the previous section. The quadratic approximation problem consists in finding a smooth vector field $\mathbf{f}$ as close as possible to a (supposedly noisy) vector field $\mathbf{g}$, by minimizing the quadratic energy

$$E(\mathbf{f}) = \int ||\mathbf{f} - \mathbf{g}||^2 + E_{reg}(\mathbf{f}) \tag{3}$$

where $E_{reg}(\mathbf{f})$ is an IDQF. (This regularization corresponds precisely to the second step of competitive P&S non-rigid registration algorithms (Cachier and Ayache, 2001)).

To find $\mathbf{f}$, we formally differentiate the approximation energy (3), and solve it in the Fourier space. Then, we deduce a vectorial convolution filter which gives the solution of (3) when applied to $\mathbf{g}$.

3.1 First Order Isotropic Filters

3.1.1 Derivatives of first-order IDQF

The derivatives of the generating elements of first-order IDQF given by (2) are reported in the following array.

Quadratic form		Derivative
$\partial_i f_j \partial_i f_j$	$\longrightarrow$	$-2\Delta\mathbf{f}$
$\partial_i f_j \partial_j f_i$	$\longrightarrow$	$-2\nabla\nabla^T\mathbf{f}$
$\partial_i f_i \partial_j f_j$	$\longrightarrow$	$-2\nabla\nabla^T\mathbf{f}$

Then, the differentiation of the approximation energy $E(\mathbf{f})$ given by (3) w.r.t $\mathbf{f}$, when E_{reg} is a first-order IDQF given by (1), gives the following differential equation:

$$\alpha\Delta\mathbf{f} + \beta\nabla\nabla^T\mathbf{f} = \mathbf{g} - \mathbf{f} \tag{4}$$

with $\alpha = 2a_1$ and $\beta = 2a_2 + 2d.a_3$. This equation (4) corresponds to a linear elastic PDE, with external forces $\mathbf{g} - \mathbf{f}$ corresponding to linear springs attracting $\mathbf{f}$ towards $\mathbf{g}$.

The aim of this minimization is regularization, so the quadratic energy should be positive. According to section 2.4, we should choose a_1, a_2 and a_3 so that $a_1 + a_2 \geq 0$, $a_1 - a_2 \geq 0$ and $a_1 + a_2 + n.a_3\gamma \geq 0$. Combining these inequalities, we find the following conditions on α and β:

$$\begin{aligned} \alpha &\geq 0 \\ \beta &\geq -\alpha \end{aligned}$$

3.1.2 Number of degrees of freedom of regularization

It appears that two out of the three generating IDQF have the same derivatives. Therefore, if the minimization of these energies uses exclusively their derivatives, there is only two degrees of freedom (parameters α and β) as for the choice of the parameters of the regularization.

This situation is similar to the scalar case. For any order of derivation, there exists several isotropic quadratic regularization energies, but all of them have the same derivatives (Nielsen et al., 1994).

For example, (Brady and Horn, 1983) showed that the squared Laplacian $(\partial_{xx}f + \partial_{yy}f)^2$ and the quadratic variation $\partial^2_{xx}f + \partial^2_{xy}f + \partial^2_{yy}f$ of a two dimensional scalar function f have the same derivatives; however, they do not lead to the same regularization: there exists functions with a squared Laplacian equal to zero, and whose quadratic variation is non zero, such as $f(x, y) = x.y$. Brady highlighted the fact that differences between these energies emerge on their derivatives on the boundary of the domain. Thus, the boundary conditions appear critical to determine the actual number of degrees of freedom of the regularization.

When using Fourier transform, the implicit boundary conditions are periodicity, i.e. we consider that opposite image borders are connected. With these assumptions, there is no other degree of freedom that those given by the derivative of the energy (3), i.e. two in the vectorial case.

3.1.3 Resolution in the Fourier Domain

The linear differential equation (4) can be solved in the Fourier space. We have the following equivalence between spatial and Fourier domains:

Spatial domain		Fourier domain
$\mathbf{f}(\mathbf{x})$	$\longleftrightarrow$	$\hat{\mathbf{f}}(\mathbf{w})$
$\Delta\mathbf{f}(\mathbf{x})$	$\longleftrightarrow$	$-(\mathbf{w}^T\mathbf{w})\hat{\mathbf{f}}(\mathbf{w})$
$(\nabla\nabla^T)\mathbf{f}(\mathbf{x})$	$\longleftrightarrow$	$-(\mathbf{w}\mathbf{w}^T)\hat{\mathbf{f}}(\mathbf{w})$

where $\mathbf{x} = (x_1, ..., x_d)$ is the canonical representation of the spatial domain, $\mathbf{w} = (w_1, ..., w_d)$ is the canonical representation of the Fourier domain, and $\hat{\mathbf{f}}$ is the Fourier transform of $\mathbf{f}$. Equation (4) transforms in the Fourier domain as:

$$\Big[\Big(1 + \alpha(\mathbf{w}^T\mathbf{w})\Big)\,\mathrm{Id} + \beta(\mathbf{w}\mathbf{w}^T)\Big]\,\hat{\mathbf{f}} = \hat{\mathbf{g}}$$

where Id is the identity matrix.

For reasons which will be explained in section 3.3.3, we replace the parameters α and β by $\alpha = \lambda$ and $\beta = \lambda\kappa$, so that λ can be identified to a regularization strength and κ to a shear strength:

$$\underbrace{\Big[\Big(1 + \lambda.(\mathbf{w}^T\mathbf{w})\Big)\,\mathrm{Id} + \lambda\kappa(\mathbf{w}\mathbf{w}^T)\Big]}_{M_1}\,\hat{\mathbf{f}} = \hat{\mathbf{g}}$$

with $\lambda \geq 0$ and $\kappa \geq -1$. To solve this equation, we have to invert the matrix M_1:

$$M_1^{-1} = \frac{1}{(1+\lambda.\mathbf{w}^T\mathbf{w})(1+\lambda(1+\kappa).\mathbf{w}^T\mathbf{w})}\left[(1+\lambda(1+\kappa).\mathbf{w}^T\mathbf{w})\mathrm{Id} - \lambda\kappa.(\mathbf{w}\mathbf{w}^T)\right] \quad (5)$$

Now, to fit $\mathbf{f}$ to $\mathbf{g}$ with the approximation energy (3), where E_{reg} is a first-order IDQF, we can proceed in three steps:

1. Compute the Fourier transform of $\mathbf{g}$;
2. Multiply this Fourier transform by the matrix function M_1^{-1} given by (5);
3. Compute the inverse Fourier transform of this product, which gives $\mathbf{f}$.

3.1.4 Impulse Response

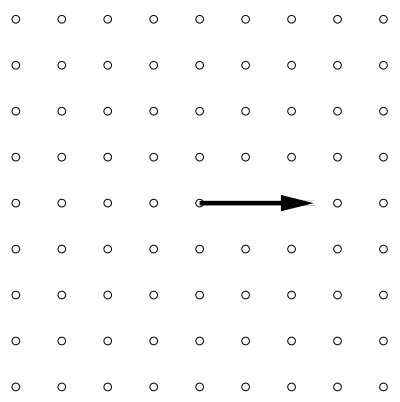

Figure 1: *In the remaining of this report, the impulse response of filters are a convolution of the filters with this vector field, which is null except for the central point which is moved to the right.*

We now show three examples of first-order isotropic regularization, depending on the sign of the cross-effect parameter κ. Here, the vector field $\mathbf{g}$ to be smoothed is a simple impulse along the horizontal axis, i.e. it is null everywhere except for the point in the middle of the image, which is moved to the right (figure 1). The results shown in figure 2 can be considered as the impulse response of the filter.

The first filter, figure 2(a), does not present any cross-effect ($\kappa = 0$) and corresponds to a membrane model. Without cross effects, horizontal lines stay straight: there is no motion along the vertical axis because the input impulse itself has no vertical component.

The second filter, figure 2(b), present cross-effects and corresponds to a standard linear elastic model ($\kappa > 0$). With $\kappa > 0$, the tissue gets closer to an incompressible model and the material is less deformed: this can be interesting for registration purposes, for example if the organs to be registered are known to behave like incompressible materials (e.g. the brain).

The last filter, figure 2(c), also has cross-effects ($\kappa < 0$), but its behavior is somewhat counter-intuitive as the impulse tends to inflate the material behind it. Although some rare materials do have this kind of behaviour, e.g. foams with negative Poisson ratio (Lakes, 1987), the choice of a negative κ for registration has probably more to do with a prior knowledge on the motion.

Note that the topology problems in the examples presented here (i.e. the overlap of a part of the material with itself near the center) are due to an arbitrary multiplicative factor used to scale the impulse response for visualization purpose.

For any value of σ or κ, there exists a discontinuity in the derivative of the impulse response, which is responsible for the sharp peak just at the point where the external force applies. In non-rigid registration, and in particular in pair-and-smooth techniques, external forces are dense, and applied at every pixel of the image, therefore such peaks may appear very frequently in the image. This is particularly annoying if the registration result is used in a first-derivative-based

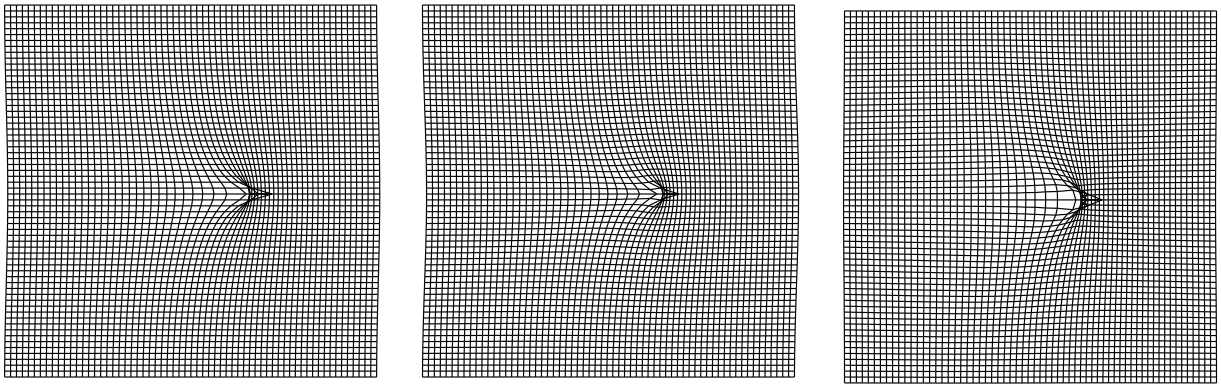

(a) $\lambda = 5$, $\kappa = 0$ (b) $\lambda = 5$, $\kappa = 0.5$ (c) $\lambda = 5$, $\kappa = -0.5$

Figure 2: *Three examples of impulse response of first-order isotropic filters without and with cross-effects*

analysis, e.g. Jacobian-based detection and segmentation (Rey et al., 1999). Therefore we will extend these vectorial filters to the second order in section 3.2

3.1.5 Isotropy vs. Rotation Invariance

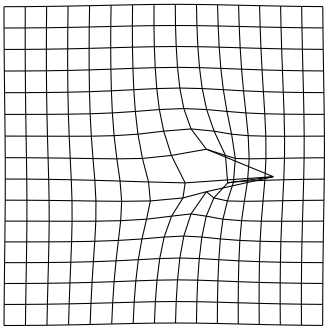

Figure 3: *Impulse response of a rotation-invariant but non-isotropic filter.*

As a remark, let us highlight here that the symmetry invariance is essential, and that rotation invariance alone, which is sufficient in the scalar case (Brady and Horn, 1983; Nielsen et al., 1994), is not sufficient anymore in the vectorial case.

In figure 3, we give the impulse response of a first-order rotation invariant but non-isotropic filter. The rotation invariance ensures that if the initial impulse is rotated, then the impulse response is rotated of the same amount. The symmetry invariance would ensure a planar symmetry of the impulse response; without this constraint, the impulse response may bend on a side or another, as if the material would present an internal torsion. These kind of effects are generally not desirable.

3.2 Second-Order Isotropic Filters

3.2.1 Derivatives of second-order IDQF

We follow the same strategy as for first-order IDQF, and begin by differentiating the basis of second-order IDQF:

Quadratic form		Derivative
$\partial_{ij}\mathbf{f}_k\partial_{ij}\mathbf{f}_k$	$\longrightarrow$	$2\Delta^2\mathbf{f}$
$\partial_{ij}\mathbf{f}_j\partial_{ik}\mathbf{f}_k$	$\longrightarrow$	$2\Delta\nabla\nabla^T\mathbf{f}$
$\partial_{ii}\mathbf{f}_j\partial_{kk}\mathbf{f}_j$	$\longrightarrow$	$2\Delta^2\mathbf{f}$
$\partial_{ij}\mathbf{f}_k\partial_{kj}\mathbf{f}_i$	$\longrightarrow$	$2\Delta\nabla\nabla^T\mathbf{f}$
$\partial_{ii}\mathbf{f}_j\partial_{kj}\mathbf{f}_k$	$\longrightarrow$	$2\Delta\nabla\nabla^T\mathbf{f}$

So the derivative of (3), where E_{reg} is a second-order IDQF, is

$$\alpha.\Delta^2\mathbf{f} + \beta.\Delta.\nabla\nabla^T\mathbf{f} = \mathbf{f} - \mathbf{g} \tag{6}$$

In section 2, we characterized positive first-order IDQF, but not positive second-order IDQF. Indeed, the conditions on coefficients a_1 through a_5 are very difficult to find in the general case. Instead, we will find a simple second-order IDQF whose derivative is the left member of (6). Conditions on this IDQF will be enough to ensure a proper regularization behavior and find acceptable ranges for α and β.

The left member of (6) is actually (proportional to) the derivative of the second-order IDQF $\alpha.\partial_{ij}f_k\partial_{ij}f_k + \beta.\partial_{ij}f_k\partial_{kj}f_i$. Its related linear function is

$$Q(T_{i,j,k}) = \alpha.T_{i,j,k}.E^{(i,j,k)} + \beta.T_{i,j,k}.E^{(i,j,k)}$$

where $E^{(i,j,k)}$ is the tensor whose only non-zero element is $E^{(i,j,k)}_{i,j,k} = 1$.

The eigentensors and eigenvalues of this linear function are

Eigentensor	Eigenvalue
$E^{(i,j,k)} - E^{(k,j,i)}, \forall(i,j,k) \in [\![1;d]\!]^3, i > k$	$\alpha - \beta$
$E^{(i,j,k)} + E^{(k,j,i)}, \forall(i,j,k) \in [\![1;d]\!]^3, i > k$	$\alpha + \beta$
$E^{(i,j,k)}, \forall(i,j) \in [\![1;d]\!]^2$	$\alpha + \beta$

There are $d^2(d-1)/2 + d^2 + d^2(d-1)/2 = d^3$ such eigenvectors, which are orthogonal, therefore there is no any other eigenvalue.

Thus, the quadratic form is positive if $\alpha + \beta \geq 0$ and $\alpha - \beta \geq 0$, i.e. if $\alpha \geq 0$ and $\beta \geq -\alpha$. There are exactly the same conditions as for the first-order case.

3.2.2 Resolution in the Fourier Domain

We have the following correspondences between the Spatial Domain and the Fourier Domain:

Spatial domain		Fourier domain
$\mathbf{f}(\mathbf{x})$	$\longleftrightarrow$	$\hat{\mathbf{f}}(\mathbf{w})$
$\Delta^2\mathbf{f}(\mathbf{x})$	$\longleftrightarrow$	$(\mathbf{w}^T\mathbf{w})^2\hat{\mathbf{f}}(\mathbf{w})$
$\Delta.\nabla\nabla^T\mathbf{f}(\mathbf{x})$	$\longleftrightarrow$	$\mathbf{w}^T\mathbf{w}(\mathbf{w}\mathbf{w}^T)\hat{\mathbf{f}}(\mathbf{w})$

Thus, in the Fourier domain, the differential equation (6) becomes:

$$\underbrace{\left[\left(1+\lambda(\mathbf{w}^T\mathbf{w})^2\right)\mathrm{Id}+\lambda\kappa(\mathbf{w}^T\mathbf{w})(\mathbf{w}\mathbf{w}^T)\right]}_{M_2}\hat{\mathbf{f}}=\hat{\mathbf{g}}$$

with $\lambda=\alpha\geq 0$ and $\kappa=\beta/\alpha\geq -1$. To solve this equation, we have to invert matrix M_2:

$$M_2^{-1}=\frac{1}{(1+\lambda.(\mathbf{w}^T\mathbf{w})^2)(1+\lambda(1+\kappa).(\mathbf{w}^T\mathbf{w})^2)}\left[(1+\lambda(1+\kappa)(\mathbf{w}^T\mathbf{w})^2)\mathrm{Id}-\lambda\kappa.(\mathbf{w}^T\mathbf{w}).\mathbf{w}\mathbf{w}^T\right]$$

This leads to an implementation identical to the scheme proposed in the first-order case, in section 3.1.3.

3.2.3 Impulse Response

In figure 4, we present the impulse response of the second-order filter for three different values of κ, one without any cross-effect ($\kappa=0$) corresponding to a thin-plate model, and two others with cross-effects. Here again, the material behaves more like a incompressible material with $\kappa>0$ and thus is less deformed. Using $\kappa<0$, the material has a non-intuitive behavior, as the impulse response is extrapolated as corresponding to an inflation of the material.

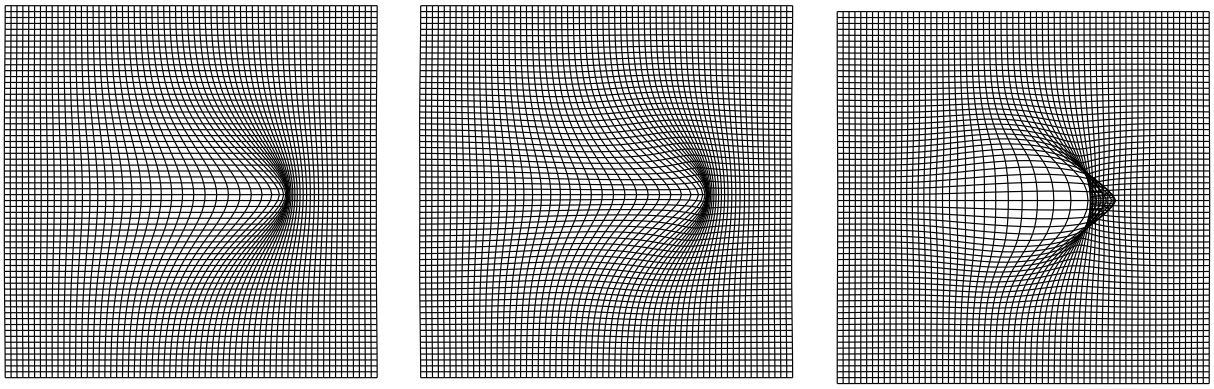

(a) $\lambda=2$, $\kappa=0$ (b) $\lambda=2$, $\kappa=0.6$ (c) $\lambda=2$, $\kappa=-0.6$

Figure 4: *Three examples of impulse response of second-order isotropic filters*

Topology problems in the case when $\kappa<0$ are due to the arbitrary multiplicative coefficient used for visualization purpose. This does not mean that choosing $\kappa<0$ will always gives topological problems.

Note that in the second-order case, impulse responses are smooth and do not have a discontinuity in their first derivative, contrary to the first-order regularization. In the context of non-rigid registration, these filters yield smoother solutions, and are more appropriate for exemple for Jacobian analysis of the motion.

3.3 Generalization

3.3.1 Higher-order isotropic filters

Given the results obtained for first and second order isotropic regularization energies, we are tempted to generalize the linear PDE to higher order regularization. Even though we did not

characterize all n-th order IDQF, we can set the PDE for the n-th order regularization as:

$$(-1)^n \left[\alpha.\Delta^n \mathbf{f} + \beta.\Delta^{n-1}.\nabla\nabla^T \mathbf{f}\right] = \mathbf{f} - \mathbf{g}$$

which is indeed isotropic, because its left member is proportional to the derivative of the following isotropic quadratic form:

$$E_n(\mathbf{f}) = \alpha.\partial_{i_1\ldots i_n} f_{i_{n+1}} \partial_{i_1\ldots i_n} f_{i_{n+1}} + \beta.\partial_{i_1\ldots i_n} f_{i_{n+1}} \partial_{i_{n+1} i_2\ldots i_n} f_{i_1} \tag{7}$$

The linear function associated to this quadratic form is

$$Q(T) = \alpha.T_{i_1,\ldots i_{n+1}} E^{(i_1,\ldots i_{n+1})} + \beta.T_{i_1,\ldots i_{n+1}}.E^{(i_{n+1},i_2,\ldots i_n,i_1)}$$

where $E^{(i_1,\ldots i_{n+1})}$ is the tensor whose only non-zero element is $E^{(i_1,\ldots i_{n+1})}_{i_1,\ldots i_{n+1}} = 1$. Its eigentensors and associated eigenvalues are (without Einstein convention):

Eigentensor	Eigenvalue
$E^{(i_1,\ldots i_{n+1})} + E^{(i_{n+1},i_2,\ldots i_n,i_1)}, \forall (i_1,\ldots,i_{n+1}) \in [\![1;d]\!]^{n+1}, i_1 > i_{n+1}$	$\alpha + \beta$
$E^{(i_1,\ldots i_{n+1})} - E^{(i_{n+1},i_2,\ldots i_n,i_1)}, \forall (i_1,\ldots,i_{n+1}) \in [\![1;d]\!]^{n+1}, i_1 > i_{n+1}$	$\alpha - \beta$
$E^{(k,i_2,\ldots i_n,k)}, \forall (k,i_2,\ldots,i_n) \in [\![1;d]\!]^{n}$	$\alpha - \beta$

We can verify, as in the second-order case, that all these tensors are orthogonal, and that they are d^n. Therefore, there exists no any other eigenvalue, and as for the first and second order regularization, we should choose $\alpha \geq 0$ and $\beta \geq -\alpha$.

We have the following correspondences between the Spatial Domain and the Fourier Domain:

Spatial domain		Fourier domain
$\mathbf{f}(\mathbf{x})$	$\longleftrightarrow$	$\hat{\mathbf{f}}(\mathbf{w})$
$\Delta^n \mathbf{f}(\mathbf{x})$	$\longleftrightarrow$	$(-1)^n (\mathbf{w}^T\mathbf{w})^n \hat{\mathbf{f}}(\mathbf{w})$
$\Delta^{n-1}(\nabla\nabla^T)\mathbf{f}(\mathbf{x})$	$\longleftrightarrow$	$(-1)^n (\mathbf{w}^T\mathbf{w})^{n-1}(\mathbf{w}\mathbf{w}^T)\hat{\mathbf{f}}(\mathbf{w})$

The differential equation becomes (setting $\alpha = \lambda$ and $\beta = \lambda\kappa$):

$$\underbrace{\left[\left(1 + \lambda.(\mathbf{w}^T\mathbf{w})^n\right) \mathrm{Id} + \lambda\kappa.(\mathbf{w}^T\mathbf{w})^{n-1}(\mathbf{w}\mathbf{w}^T)\right]}_{M_n} \hat{\mathbf{f}} = \hat{\mathbf{g}}$$

To solve this equation, we have to invert the matrix M_n:

$$M_n^{-1} = \frac{1}{1 + \lambda.(\mathbf{w}^T\mathbf{w})^n}\mathrm{Id} - \frac{\lambda\kappa(\mathbf{w}^T\mathbf{w})^{n-1}}{(1 + \lambda.(\mathbf{w}^T\mathbf{w})^n)(1 + \lambda(1+\kappa).(\mathbf{w}^T\mathbf{w})^n)}\mathbf{w}\mathbf{w}^T \tag{8}$$

As previously, the regularization is done by multiplying the Fourier transform of the vector field by the matrix M_n^{-1}.

3.3.2 Multi-order filters

A regularization energy may include several (or even all) orders of derivation. We can consider regularization energies that are linear combinations of our previous isotropic energies (7)

$$\sum_{n=1}^{\infty} \alpha_n . \partial_{i_1 \dots i_n} f_{i_{n+1}} \partial_{i_1 \dots i_n} f_{i_{n+1}} + \beta_n . \partial_{i_1 \dots i_n} f_{i_{n+1}} \partial_{i_{n+1} i_2 \dots i_n} f_{i_1} \tag{9}$$

The regularization PDE is

$$\sum_{n=1}^{\infty} (-1)^n \left[\alpha_n . \Delta^n \mathbf{f} + \beta_n . \Delta^{n-1} . \nabla \nabla^T \mathbf{f} \right] = \mathbf{f} - \mathbf{g}$$

with two scalar $\alpha_n \geq 0$ and $\beta_n \geq -\alpha_n$ to choose per order of derivation. There are two degrees of freedom per order of differentiation, corresponding approximately to its strength and its shear. In the Fourier domain, the previous PDE becomes

$$\underbrace{\left[\left(1 + \sum_{n=1}^{\infty} \alpha_n (\mathbf{w}^T \mathbf{w})^n \right) \mathrm{Id} + \sum_{n=1}^{\infty} \beta_n (\mathbf{w}^T \mathbf{w})^{n-1} (\mathbf{w} \mathbf{w}^T) \right]}_{M} \hat{\mathbf{f}} = \hat{\mathbf{g}}$$

As previously, one should invert matrix M and apply it to the Fourier transform of $\mathbf{g}$ to obtain the solution.

3.3.3 A note on the regularization strength

Energies (9) are designed for regularization. Therefore, we should be able to control their weight relatively to another energy, typically a fitting distance, *via* a regularization parameter λ. Now, what influence should have λ on each order of differentiation?

In the case of quadratic approximation, choosing λ as a global multiplicative factor:

$$\lambda . E_{reg}(\mathbf{f}) = \lambda . \sum_{n=1}^{\infty} \alpha_n . \partial_{i_1 \dots i_n} f_{i_{n+1}} \partial_{i_1 \dots i_n} f_{i_{n+1}} + \beta_n . \partial_{i_1 \dots i_n} f_{i_{n+1}} \partial_{i_{n+1} i_2 \dots i_n} f_{i_1} \tag{10}$$

gives counterintuitive results, because λ changes the shape of the impulse response of (10), instead of just rescaling it.

If we want to extract from the parameters α_n and β_n a regularization strength λ that corresponds to a scale factor of the impulse response, we should choose

$$E_{reg}(\mathbf{f}, \lambda) = \sum_{n=1}^{\infty} \lambda^n \left[\alpha_n . \partial_{i_1 \dots i_n} f_{i_{n+1}} \partial_{i_1 \dots i_n} f_{i_{n+1}} + \beta_n . \partial_{i_1 \dots i_n} f_{i_{n+1}} \partial_{i_{n+1} i_2 \dots i_n} f_{i_1} \right]$$

Therefore, in the general case, it seems better not to write the regularization parameter λ as a multiplicative factor of the energy but rather as a parameter of the regularization energy itself. However, if the regularization energy uses only one order of differentiation, which is quite frequent in non-rigid registration, both approaches are of course equivalent, and λ can be written as a multiplicative coefficient of the energy.

3.4 Separable Isotropic Filters

In this section, we are interested in finding isotropic vectorial filters similar to the previous filters, with the additional constraint that they should be separable, so that they can be applied numerically very efficiently in the real domain, without using Fourier transforms.

3.4.1 Definitions

Definition 6 (Isotropic Filters) *A scalar filter $f(\mathbf{x}) : \mathbb{R}^d \to \mathbb{R}$ is isotropic if it is invariant by rotations and symmetries, i.e. if*

$$f(R^T\mathbf{x}) = f(\mathbf{x}) \quad \forall R \in O(d)$$

A vector filter is isotropic if its kernel $F(\mathbf{x}) = F(x_1, ..., x_d) : \mathbb{R}^d \to \mathcal{M}_d$ is invariant by rotation and symmetries:

$$R.F(R^T\mathbf{x}).R^T = F(\mathbf{x}) \quad \forall R \in O(d)$$

An isotropic scalar filter f depends only on radial distance: $f(\mathbf{x}) = g(\mathbf{x}^T\mathbf{x})$. This is not true anymore for isotropic vector filters.

Definition 7 (Separable Filters) *A scalar kernel $f(\mathbf{x}) = f(x_1, ..., x_d) : \mathbb{R}^d \to \mathbb{R}$ is separable if there exist d functions f_k, $k \in [\![1; d]\!]$, such that:*

$$f(\mathbf{x}) = f_1(x_1).f_2(x_2)...f_d(x_d) = \prod_{k=1}^{d} f_k(x_k)$$

A vector filter $F(\mathbf{x}) = F(x_1, ..., x_d) : \mathbb{R}^d \to \mathcal{M}_d$ is separable is there exists d^3 functions $f_k^{(i,j)}$, $(i, j, k) \in [\![1; d]\!]^3$, such that

$$F(\mathbf{x}) = \begin{pmatrix} \prod_{k=1}^d f_k^{(1,1)} & \prod_{k=1}^d f_k^{(1,2)} & \cdots & \prod_{k=1}^d f_k^{(1,d)} \\ \prod_{k=1}^d f_k^{(2,1)} & & & \vdots \\ \vdots & & & \vdots \\ \prod_{k=1}^d f_k^{(d,1)} & \cdots & \cdots & \prod_{k=1}^d f_k^{(d,d)} \end{pmatrix}$$

This property of separability is very interesting from a numerical point of view, because a n-D convolution with a separable filter can be achieved as a sequence of 1-D convolutions, for which a number of fast techniques exists such as recursive filtering.

The choice of separable filters is drastically restricted if we also impose the isotropy property. For scalars, it is known that the only isotropic separable kernels are the family of Gaussians (Kannappan and Sahoo, 1992). However, for the best of our knowledge, there is no similar theorem for vector filters. We propose the following result, easy to verify:

Proposition 1 *The vector filter $G_{\sigma,\kappa}$ defined by*

$$G_{\sigma,\kappa}(\mathbf{x}) = \frac{1}{\left(\sigma\sqrt{2\pi}\right)^d(1+\kappa)}(Id_d + \frac{\kappa}{\sigma^2}.\mathbf{x}.\mathbf{x}^T).e^{-\frac{\mathbf{x}^T\mathbf{x}}{2\sigma^2}} \tag{11}$$

is separable and isotropic.

The normalization coefficient $\left(\sigma\sqrt{2\pi}\right)^d(1+\kappa)$ is chosen so that a constant vector field is unchanged by convolution with $G_{\sigma,\kappa}$. Equivalently, the integral of the diagonal elements of the matrix $G_{\sigma,\kappa}(\mathbf{x})$ should be equal to 1. As previously, the coefficient κ is linked to the degree of shear we expect in the material. Note that when κ is set to zero, the matrix $G_{\sigma,0}$ becomes diagonal, and we obtain a classical Gaussian filtering, independently on each component of the vector field.

There exist separable isotropic filters that are not part of this previous family, as this filter in 2D:

$$\frac{1}{\left(\sigma\sqrt{2\pi}\right)^2(1-\kappa)}\begin{pmatrix} 1-\kappa.y^2/\lambda & \kappa.x.y/\lambda \\ \kappa.x.y/\lambda & 1-\kappa.x^2/\lambda \end{pmatrix}.e^{-\frac{x^2+y^2}{2\lambda}}$$

We think that such counter examples are possible only in two dimensions and cannot be generalized in higher dimension. The filters $G_{\sigma,\kappa}$ given by (11) are probably the only separable isotropic filters in dimension greater or equal to 3, but this has yet to be proven.

3.4.2 Computation with classical Gaussian filters

Proposition 2 *If we note* $G_\sigma(\mathbf{x}) = \exp(-\mathbf{x}^T\mathbf{x}/(2\sigma^2))/(\sigma\sqrt{2\pi})^d$ *the normalized, d-dimensional scalar Gaussian kernel, and* $\mathcal{H}G_\sigma$ *the Hessian matrix consisting of its second-order derivatives, the following relation holds:*

$$G_{\sigma,\kappa}(\mathbf{x}) = G_\sigma(\mathbf{x}).Id + \frac{\sigma^2\kappa}{1+\kappa}\mathcal{H}G_\sigma(\mathbf{x})$$

Because $G_\sigma(\mathbf{x})$.Id and $\mathcal{H}G_\sigma(\mathbf{x})$ are also separable, the convolution with $G_{\sigma,\kappa}$ can be computed as a weighted sum of convolutions with a one-dimensional Gaussian, and its first and second derivatives. There exists many efficient techniques to implement these filters. Here, we have chosen Deriche's recursive filters (Deriche, 1993), which have a computation time independent of the size of the Gaussian kernel.

3.4.3 Impulse Response

Figure 11 shows the impulse responses of the separable isotropic filter (11) for three different values of parameter κ. With a κ set to zero (figure 5(a)), we obtain a classical scalar Gaussian filter which is applied on each component separately. Setting κ to a positive or negative value enables cross effects and yields to the same physical interpretation as for the previous first- and second-order filters.

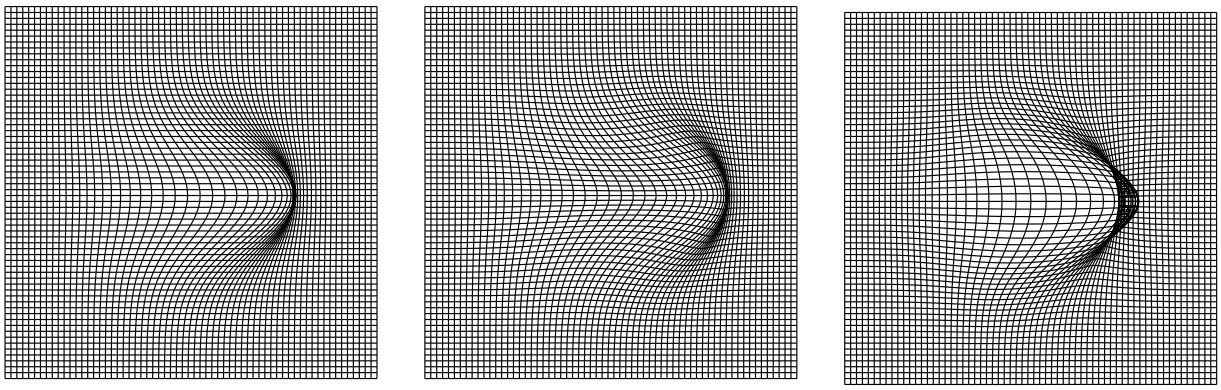

(a) $\sigma = 8$, $\kappa = 0$ (b) $\sigma = 8$, $\kappa = 1/8$ (c) $\sigma = 8$, $\kappa = -1/8$

Figure 5: *Impulse responses of different separable isotropic vector filters* $G_{\sigma,\kappa}$ *(11) generalizing the classical scalar Gaussian filtering to vectors.*

3.5 An application to image registration

In the experiment reported in figure 6, two circles have been moved apart. They have been registered with `PASHA` (Cachier and Ayache, 2001), a competitive pair-and-smooth non-rigid registration algorithm, using the separable isotropic filters described in section 3.4 for the regularization step. We have run the registration without ($\kappa = 0$) and with cross-effects ($\kappa > 0$).

Without cross-effects, horizontal lines stay horizontal outside the circles. Especially, there is no noticeable vertical deformation between the circles. Choosing $\kappa > 0$ gives a more realistic extrapolation of the motion, as the material between both circles is bending towards the center. Depending on prior knowledge on the material, this latter behaviour may be more appropriate.

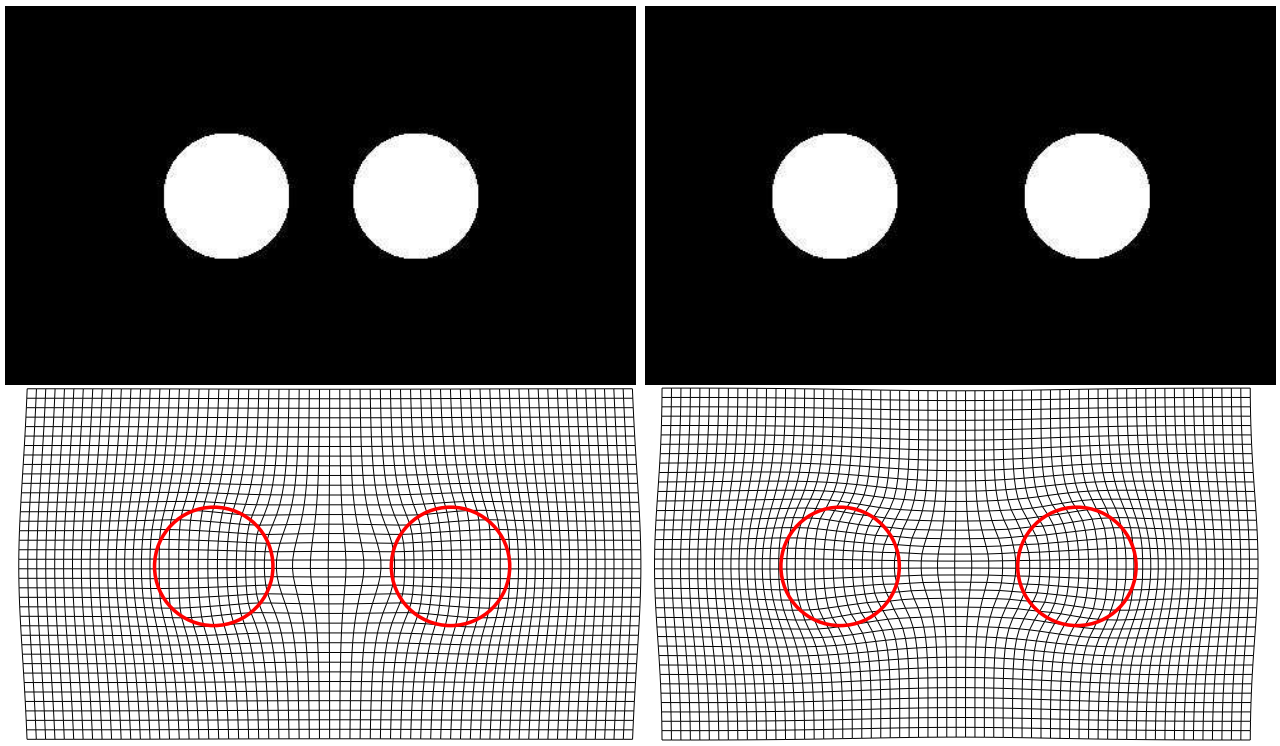

Figure 6: ***Up:*** *Two circles initially closed to each other are moved far apart.* ***Down:*** *Result of registration, without (left) and with (right) cross-effect filtering. Without cross-effects, horizontal lines stay horizontal outside the circles, and there is no noticeable vertical deformation. With cross-effects, the material between the circles is compressing vertically to compensate the horizontal dilatation.*

4 Vectorial Basis Functions for Feature Point Matching

This section has multiple goals. First, we want to generalize thin-plate splines and other radial-basis functions in the case of vector interpolation, using the isotropic energies and PDEs developed previously. Similarly to the filters obtained in section 3, we obtain interpolation kernels with cross-effects that are no more radial and cannot be applied on each component independently. Then, we merge the dense vectorial approximation problem of section 3 with the sparse vectorial approximation presented here to obtain an hybrid approximation scheme.

This is of high interest for merging intensity and geometrical features in non-rigid registration algorithms (Cachier et al., 2001).

4.1 Interpolation and Approximation for Scalars and Vectors

4.1.1 The scalar case

The scalar interpolation problem can be defined as follows: given a set of p points $\mathbf{x}_i \in \mathbb{R}^d$ and p values $f_i \in \mathbb{R}$, find a functional f that minimizes some regularization energy $E_{reg}(f)$ under the constraint that $f(\mathbf{x}_i) = f_i$, $\forall i \in [\![1; p]\!]$. This interpolation problem assumes that there are no error on the measure of the values f_i.

The scalar approximation problem is close to the previous one, but this time the f_i may be corrupted by noise, and thus f is allowed to have at $\mathbf{x}_i$ a value different yet close to the initial guess f_i. The optimal solution f^* to approximate f_i is chosen as the solution of the optimization problem:

$$f^* = \arg\min_f \sum_i (f_i - f(\mathbf{x}_i))^2 + \lambda E_{reg}(f)$$

The approximation problem tends toward an interpolation problem as $\lambda \to 0$. (Besides, as discussed in section 3.3.3, λ is not necessarily a multiplicative factor of the regularization energy).

4.1.2 The vectorial case

Given two sets of points $\mathbf{x}_i$ and $\mathbf{y}_i$, the vector interpolation problem consists in finding a transformation T which minimizes a regularization energy $E_{reg}(T)$ under the constraint that $T(\mathbf{x}_i) = \mathbf{y}_i$. As for the vectorial approximation problem, it seeks an approximation T^* which is solution of

$$T^* = \arg\min_T \sum_i ||\mathbf{y}_i - T(\mathbf{x}_i)||^2 + \lambda E_{reg}(T)$$

There are more elaborated approximation problems, where for example the isotropic distance $||\mathbf{y}_i - T(\mathbf{x}_i)||^2$ is replaced by an anisotropic distance depending on the index i (Rohr et al., 1999).

4.2 Scalar Laplacian Splines

When E_{reg} is a quadratic energy, there exists a closed form solution for the interpolation and approximation of scalars (Duchon, 1976). In both cases, the solution has the following form:

$$f(\mathbf{x}) = p(\mathbf{x}) + \sum_i \alpha_i s(\mathbf{x} - \mathbf{x}_i) \tag{12}$$

where $p(\mathbf{x})$ is a polynomial in the kernel of E_{reg}, i.e. $E_{reg}(p) = 0$, and s is a function, commonly called spline, that depends only on E_{reg} and the dimension of the space where points $\mathbf{x}_i$ and $\mathbf{y}_i$ are located

When E_{reg} is the n-th order regularization energy $\partial_{i_1 \ldots i_n} f \partial_{i_1 \ldots i_n} f$, the spline s belongs to the family of the Laplacian splines s_n, that are solution of the PDE

$$(-1)^n \Delta^n s_n = \delta$$

or, more generally, $\Delta^n s = \alpha\delta$, where α is an appropriate constant multiplicative factor introduced only to simplify the expression of s; the introduction of this multiplicative factor has no consequence on the solution, which remain the same – the coefficients α_i of (12) are simply divided by $(-1)^n\alpha$. This linear PDE can be solved, and there exists closed-form formulas for s (Duchon, 1976). The most famous of these splines is perhaps the second-order Laplacian spline s_2, or thin plate spline, whose equation is $r^2 \ln r$ in 2D and $|r|$ in 3D.

The coefficients α_i as well as the coefficients of the polynomial p are found by resolving a set of linear equations, which requires the inversion of a matrix of size $(p+n)\times(p+n)$, where p is the number of points to be interpolated or approximated, and n the number of coefficients in the multivariate polynomial p. We give an example in the case of thin plate spline interpolation and approximation.

Example: Thin Plate Spline Interpolation

The thin plate spline is the Laplacian spline of order 2, related to the bending energy $E_2(\mathbf{f}) = \partial_{ij}f\partial_{ij}f$. The polynomial p in the formula (12) is then a polynomial of order 1, i.e. an affine function.

The function f whose values on a set of p points $\mathbf{x}_i \in \mathbb{R}^d$ is f_i and that minimizes the bending energy E_2 is

$$f(\mathbf{x}) = p0 + (p_1, ..., p_d).\mathbf{x} + \sum_{i=1}^{p} \alpha_i s_2(\mathbf{x} - \mathbf{x}_i)$$

where the unknowns $\mathbf{a} = (\alpha_1, ..., \alpha_p, p_0, p_1, ..., p_d)^T$ are solution of the linear equation

$$\left(\begin{array}{c|c} W & X^T \\ \hline X & 0 \end{array}\right).\mathbf{a} = \left(\begin{array}{c} \mathbf{f} \\ \hline 0 \end{array}\right) \tag{13}$$

with W being the $p \times p$ matrix

$$W = (s_2(\mathbf{x}_i - \mathbf{x}_j)) = \begin{pmatrix} s_2(\mathbf{x}_1 - \mathbf{x}_1) & s_2(\mathbf{x}_1 - \mathbf{x}_2) & \cdots & s_2(\mathbf{x}_1 - \mathbf{x}_p) \\ s_2(\mathbf{x}_2 - \mathbf{x}_1) & \ddots & & \vdots \\ \vdots & & \ddots & \vdots \\ s_2(\mathbf{x}_p - \mathbf{x}_1) & \cdots & \cdots & s_2(\mathbf{x}_p - \mathbf{x}_p) \end{pmatrix}$$

X the $(d+1) \times p$ matrix

$$X = \begin{pmatrix} 1 & \cdots & 1 \\ \mathbf{x}_1 & \cdots & \mathbf{x}_p \end{pmatrix}$$

and $\mathbf{f}$ the p-vector

$$\mathbf{f} = (f_1, ..., f_p)^T$$

In equation (13), the condition $X.(\alpha_1 ... \alpha_p)^T = 0$ can be seen as a constraint on the coefficients α_i so that the sum $\sum_{i=1}^{p} \alpha_i s_2(\mathbf{x} - \mathbf{x}_i)$ remains bounded. Indeed, when $\mathbf{x}$ becomes large,

$$\sum_i \alpha_i ||\mathbf{x} - \mathbf{x}_i|| \ln ||\mathbf{x} - \mathbf{x}_i|| = ||\mathbf{x}|| \ln ||\mathbf{x}|| \left(\sum_i \alpha_i\right) - \frac{\mathbf{x}^T}{||\mathbf{x}||}\left(\sum_i \alpha_i \mathbf{x}_i\right) + O(1)$$

Therefore, to obtain a bounded solution, we should cancel the two sums in the right member of the previous equation, i.e. set $\sum_i \alpha_i$ and $\sum_i \alpha_i \mathbf{x}_i$ to zero.

When the f_i are noisy, f can be sought to minimize the following approximation energy:

$$E(f) = \sum_i (f(\mathbf{x}_i) - f_i)^2 + \sigma E_2(f)$$

The vector of the unknown coefficients $\mathbf{a}$ is then solution of the equation

$$\left(\begin{array}{c|c} W + \sigma.\mathrm{Id} & X^T \\ \hline X & 0 \end{array}\right).\mathbf{a} = \left(\begin{array}{c} \mathbf{f} \\ \hline 0 \end{array}\right)$$

4.3 Vectorial Laplacian Splines

For vector interpolation and approximation, the most common solution in the field of non-rigid registration consists in interpolating or approximating every component independently, and thus to split the problem of n-dimensional vector fitting into n problems of scalar fitting. Thus, radial basis functions like the thin-plate spline are used for each component independently.

A notable exception is the elastic body spline of (Davis et al., 1997), which is based on linear elasticity. Unfortunately, the exact interpolation kernel of linear elasticity is ill-defined as it tends toward infinity at its center.

For vector interpolation or approximation problems, we propose to generalize the n-th order Laplacian spline by using the isotropic quadratic energies (7) of section 3.3.1:

$$E_n(\mathbf{f}) = \partial_{i_1 \ldots i_n}\mathbf{f}_{i_{n+1}} \partial_{i_1 \ldots i_n}\mathbf{f}_{i_{n+1}} + \kappa.\partial_{i_1 i_2 \ldots i_n}\mathbf{f}_{i_{n+1}} \partial_{i_{n+1} i_2 \ldots i_n}\mathbf{f}_{i_1}$$

If we note S_n the matrix solution of

$$(-1)^n \left[\Delta^n S_n + \kappa \Delta^{n-1} \nabla \nabla^T S_n\right] = \delta.\mathrm{Id} \tag{14}$$

then the solution $\mathbf{f}$ of the vector interpolation of approximation problem has the following form

$$\mathbf{f}(\mathbf{x}) = \mathbf{p}(\mathbf{x}) + \sum_i S_n(\mathbf{x} - \mathbf{x}_i)\boldsymbol{\alpha}_i \tag{15}$$

where $\mathbf{p}$ is a vector polynomial such that $E(\mathbf{p}) = 0$, and $\boldsymbol{\alpha}_i \in \mathbb{R}^d$ are appropriate coefficients, found by resolving a system of linear equations.

Closed-form formulas

As in the scalar case, it is possible to get closed-form formulas for S_n. Getting into the Fourier domain, the PDE (14) becomes

$$\left[(\mathbf{w}^T\mathbf{w})^n \mathrm{Id} + \kappa(\mathbf{w}^T\mathbf{w})^{n-1}\mathbf{w}\mathbf{w}^T\right] \hat{S}_n = \mathrm{Id}$$

and we find that

$$\hat{S}_n = \frac{1}{(\mathbf{w}^T\mathbf{w})^n}\mathrm{Id} - \frac{\kappa}{(1+\kappa)(\mathbf{w}^T\mathbf{w})^{n+1}}\mathbf{w}\mathbf{w}^T$$

The Fourier transform of the scalar Laplacian spline s_n is precisely $\frac{1}{(\mathbf{w}^T\mathbf{w})^n}$. Thus, we can express S_n as a function of s_n and s_{n+1}:

$$S_n = s_n \mathrm{Id} + \frac{\kappa}{1+\kappa}\mathcal{H}s_{n+1}$$

where $\mathcal{H}s_{n+1}$ is the Hessian matrix of s_{n+1}.

Example: Vectorial Thin Plate Spline Interpolation

Up to a multiplicative coefficient, the 2-D second-order Laplacian spline (or thin plate spline) is $s_2(x,y) = r^2 \ln r^2$, and the 2-D third-order Laplacian spline is $s_3(x,y) = r^4 \ln r^2$ (Duchon, 1976), where $r^2 = x^2 + y^2$.

The Hessian matrix of s_3 is

$$\mathcal{H}s_3 = 2 \begin{pmatrix} 2(3x^2+y^2)\ln r^2 + 7x^2 + y^2 & 2xy(2\ln r^2 + 3) \\ 2xy(2\ln r^2 + 3) & 2(3y^2+x^2)\ln r^2 + 7y^2 + x^2 \end{pmatrix}$$

Thus, S_2 is of the form

$$S_2 = \begin{pmatrix} r^2 \ln r^2 + \frac{\kappa}{1+\kappa}\left[2(3x^2+y^2)\ln r^2 + 7x^2 + y^2\right] & 2\frac{\kappa}{1+\kappa}xy(2\ln r^2 + 3) \\ 2\frac{\kappa}{1+\kappa}xy(2\ln r^2 + 3) & r^2 \ln r^2 + \frac{\kappa}{1+\kappa}\left[2(3y^2+x^2)\ln r^2 + 7y^2 + x^2\right] \end{pmatrix}$$

Figure 7 compares the basis function associated to this matrix and the scalar thin plate spline.

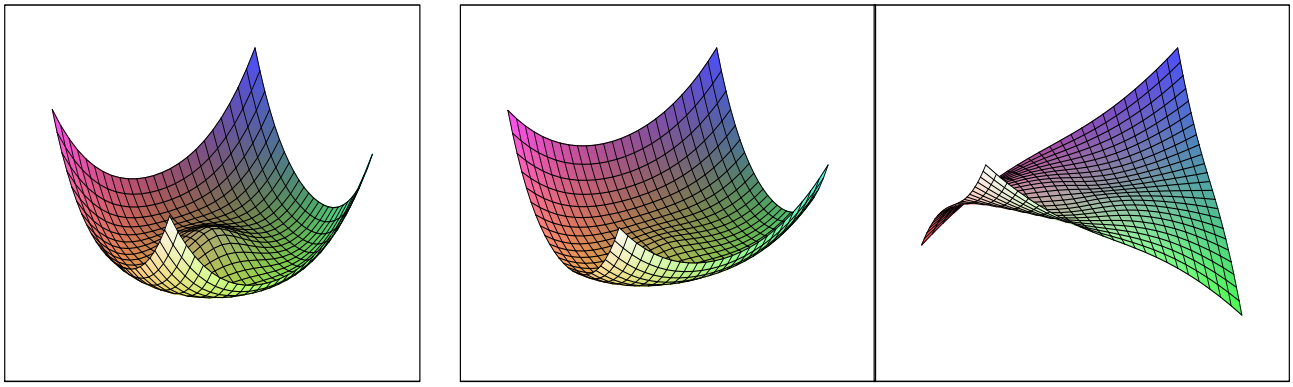

Figure 7: *Interpolating splines:* ***Left:*** *The 2D scalar thin-plate spline.* ***Right:*** *The x- and y-component of a 2D vectorial thin-plate spline.*

In figure 8, we compare the results of the interpolation of motion using scalar and vectorial thin plate splines. In the original position (figure 8(a)), four points are placed at each corner of a square. Then the upper point, in red, is forced to move to the center of the square.

The interpolation using both methods are given in figure 8(b) and 8(c). The scalar thin-plate spline interpolation applied on each component independently, in figure 8(b), do not present any horizontal motion, and thus vertical lines remains straight. It possess a strong accumulation of matter just under the point that has been moved. The vectorial Laplacian spline interpolation, in figure 8(c), is more realistic because of the horizontal motion, which enables the motion to be less strained, especially under the red point where the previous accumulation of matter has disappear.

4.4 Merging Filters and Basis Function

In section 3 we have seen that the continuous approximation problem

$$\min \int ||T - C||^2 + E_{reg}(T)$$

where $E_{reg}(T)$ is an IDQF, has a closed-form solution using convolution. In section 4.3 we have seen that the discrete approximation problem

$$\min \sum_i ||T(\mathbf{x}_i) - C(\mathbf{x}_i)||^2 + E_{reg}(T)$$

has a closed-form solution which is a linear combination of vectorial basis functions, whose multiplicative coefficients are found by resolving a set of linear equations.

Now, we merge the two previous problems: we search for a vector field T that should approximate both a continuous function C_1, and a set of discrete pairings C_2. The energy to minimize is thus

$$E(T) = \int ||T - C_1||^2 + \gamma \sum_i ||T(\mathbf{x}_i) - C_2(\mathbf{x}_i)||^2 + E_{reg}(T)$$

We show in appendix B that T has a very interesting closed form formula: it is a linear combination of a smoothed vector field and a sum of splines

$$T(\mathbf{x}) = K * C_1(\mathbf{x}) + \sum_i K(\mathbf{x} - \mathbf{x}_i)\boldsymbol{\alpha}_i \tag{16}$$

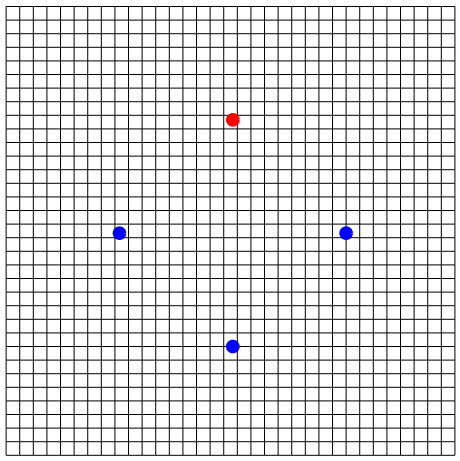

(a) Original Position

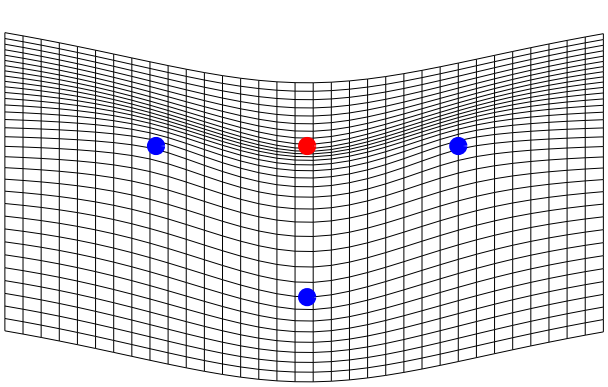

(b) Deformation using thin plate splines

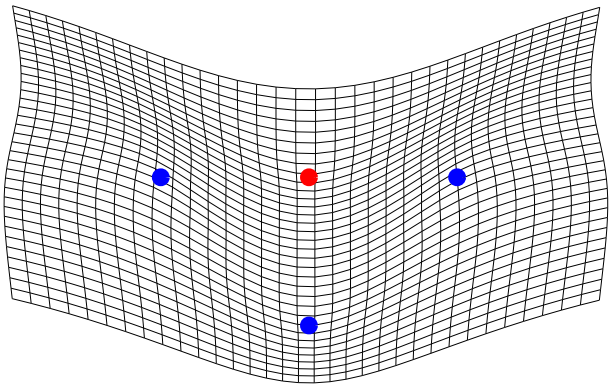

(c) Deformation using vectorial thin plate splines

Figure 8: *Interpolation of motion using splines. The three green circles stay at their original position, while the red circle comes down to the center of the square. Without cross effects, vertical lines remain vertical and straigth, and present a strong accumulation of matter in front of the translated point. When using cross-effect, the matter is less deformed and has a more physical motion.*

where K is the smoothing kernel associated to E_{reg}, as those found in section 3, and $\boldsymbol{\alpha}_i \in \mathbb{R}^d$ are coefficients found by resolving a set of linear equations. The same kernel is used both as a smoothing kernel to smooth C_1, and as a spline to approximate the sparse correspondences C_2. Contrary to the vectorial Laplacian splines of section 4.3, though, these splines are bounded and decrease toward zero at infinity.

This formulation can be very useful in the context of non-rigid registration, when one wants to add point feature matching to and intensity-based registration : the similarity measure gives dense correspondences C_1, while geometric constraint gives sparse correspondences C_2. A non-rigid motion can thus be estimated from these two sets using equation (16). An example of this application to multipatient brain comparison using intensity and sulci matching can be found in (Cachier et al., 2001).

5 Conclusion

In this report we introduced some new techniques for regularizing vectorial problems. We first studied isotropic quadratic energies, and then used these energies to deduce vector filters and splines to approximate respectively a dense and sparse vector field. We also introduced a separable vector filter that generalizes Gaussian filtering to vectors and enables a particularly efficient smoothing, using recursive filtering.

The original feature of vector regularization is the possibility to have cross-effects between components, which is not possible using standard scalar regularization on each component separately. This new parameter makes it possible to more finely tune the solution of our problem, in the context of non-rigid registration for example, depending on our prior knowledge.

A Second-Order IDQF

According to Theorem 1, the 15 quadratic forms that generate the set of second-order IDQF are

$\partial_{ii}f_j\partial_{jk}f_k$	(17)	$\partial_{ii}f_j\partial_{kj}f_k$	(22)	$\partial_{ii}f_j\partial_{kk}f_j$	(27)
$\partial_{ij}f_i\partial_{jk}f_k$	(18)	$\partial_{ij}f_i\partial_{kj}f_k$	(23)	$\partial_{ij}f_i\partial_{kk}f_j$	(28)
$\partial_{ij}f_j\partial_{ik}f_k$	(19)	$\partial_{ij}f_k\partial_{ij}f_k$	(24)	$\partial_{ij}f_k\partial_{ik}f_j$	(29)
$\partial_{ij}f_j\partial_{ki}f_k$	(20)	$\partial_{ij}f_k\partial_{ji}f_k$	(25)	$\partial_{ij}f_k\partial_{ki}f_j$	(30)
$\partial_{ij}f_j\partial_{kk}f_i$	(21)	$\partial_{ij}f_k\partial_{jk}f_i$	(26)	$\partial_{ij}f_k\partial_{kj}f_i$	(31)

Because we suppose that the derivation commutes with itself, some of these 15 quadratic forms are equal. It is straightforward to see that (17)=(22), (18)=(23), (19)=(20), (24)=(25), (26)=(31) and (29)=(30). Renaming $i \to j$ and $j \to i$, we also find (19)=(23), (21)=(28) and (29)=(31). We now have only 6 quadratic forms:

$\partial_{ij}f_j\partial_{ik}f_k$	(32)	$\partial_{ij}f_k\partial_{ij}f_k$	(34)	$\partial_{ij}f_i\partial_{kk}f_j$	(36)
$\partial_{ii}f_j\partial_{kj}f_k$	(33)	$\partial_{ii}f_j\partial_{kk}f_j$	(35)	$\partial_{ij}f_k\partial_{kj}f_i$	(37)

Now, because the multiplication commutes, two of these 6 quadratic forms are also equal. Renaming $k \to i$ and $i \to k$, we see that (33)=(36). We finally have only 5 independent quadratic forms:

$$\partial_{ij}f_j\partial_{ik}f_k \qquad \partial_{ii}f_j\partial_{kj}f_k \qquad \partial_{ij}f_k\partial_{ij}f_k \qquad \partial_{ii}f_j\partial_{kk}f_j \qquad \partial_{ij}f_k\partial_{kj}f_i$$

B Merging Filters and Basis Function

We now focus on the problem where T should fit both a continuous function C_1, and a set of discrete pairings C_2. The energy to minimize is thus

$$E(T) = \int ||T - C_1||^2 + \gamma \sum_i ||T(\mathbf{x}_i) - C_2(\mathbf{x}_i)||^2 + E_{reg}(T)$$

Using the Fourier transform, we rewrite the previous energy:

$$E(T) = \int ||\hat{T} - \hat{C}_1||^2 + \gamma \sum_i ||T(\mathbf{x}_i) - C_2(\mathbf{x}_i)||^2 + \int P(\mathbf{w}).||\hat{T}||^2$$

where $P(\mathbf{w})$ is a polynomial matrix related to the IDQF E_{reg}, and which is a linear combination of the terms $\lambda(\mathbf{w}^T\mathbf{w})^n + \lambda\kappa(\mathbf{w}^T\mathbf{w})^{n-1}\mathbf{w}\mathbf{w}^T$ if E_{reg} is on the form (9) (see section 3). Since $T(\mathbf{x}_i) = \int \hat{T}(\mathbf{w}) \exp(2\pi i.\mathbf{w}^T\mathbf{x}_i)$, the formal differentiation of this energy w.r. to $\hat{T}$ leads to

$$(\hat{T} - \hat{C}_1) + \gamma \sum_i (T(\mathbf{x}_i) - C_2(\mathbf{x}_i)) \exp(-2\pi i\mathbf{w}^T\mathbf{x}_i) + P(\mathbf{w}).\hat{T} = 0$$

The solution of this equation is

$$\hat{T} = M^{-1}\hat{C}_1 + \gamma \sum_i \exp(-2\pi i\mathbf{w}^T\mathbf{x}_i) M^{-1}(C_2(\mathbf{x}_i) - T(\mathbf{x}_i))$$

where M^{-1} is the invert matrix of $M = \mathrm{Id} + P(\mathbf{w})$, with the same notation of section 3.

Let us note K the inverse Fourier transform of M^{-1}. In the real domain, the first term $M^{-1}\hat{C}_1$ transforms as $K * C_1$, as in section 3. Since M^{-1} is the Fourier transform of $K(\mathbf{x})$, $\exp(-2\pi i \mathbf{w}^T \mathbf{x}_i) M^{-1}$ is the Fourier transform of $K(\mathbf{x} - \mathbf{x}_i)$, so the second term transforms as $\gamma \sum_i K(\mathbf{x} - \mathbf{x}_i)(C_2(\mathbf{x}_i) - T(\mathbf{x}_i))$. The solution to this approximation problem is thus of the form

$$T(\mathbf{x}) = K * C_1(\mathbf{x}) + \sum_i K(\mathbf{x} - \mathbf{x}_i)\boldsymbol{\alpha}_i$$

where $\boldsymbol{\alpha}_i = \gamma(C_2(\mathbf{x}_i) - T(\mathbf{x}_i)) \in \mathbb{R}^d$ is a set of multiplicative coefficient that solve the set of equation:

$$K * C_1(\mathbf{x}_i) + \sum_j K(\mathbf{x}_i - \mathbf{x}_j)\boldsymbol{\alpha}_j = C_2(\mathbf{x}_i) - \boldsymbol{\alpha}_i/\gamma \qquad \forall i \in [\![1; p]\!]$$

Let us note $\boldsymbol{\alpha}$ the vector of size $d.p$ of all the coefficient

$$\boldsymbol{\alpha} = (\boldsymbol{\alpha}_1^T, ..., \boldsymbol{\alpha}_p^T)^T$$

Let us note W the $(d.p) \times (d.p)$ matrix

$$W = (K(\mathbf{x}_i - \mathbf{x}_j)) = \begin{pmatrix} K(\mathbf{x}_1 - \mathbf{x}_1) & K(\mathbf{x}_1 - \mathbf{x}_2) & \cdots & K(\mathbf{x}_1 - \mathbf{x}_p) \\ K(\mathbf{x}_2 - \mathbf{x}_1) & \ddots & & \vdots \\ \vdots & & \ddots & \vdots \\ K(\mathbf{x}_p - \mathbf{x}_1) & \cdots & \cdots & K(\mathbf{x}_p - \mathbf{x}_p) \end{pmatrix}$$

Finally, let us note $\boldsymbol{\beta}$ the vector of size $d.p$

$$\boldsymbol{\beta} = ((C_2(\mathbf{x}_1) - K * C_1(\mathbf{x}_1))^T, ..., (C_2(\mathbf{x}_p) - K * C_1(\mathbf{x}_p))^T$$

Then to find the coefficients α_i, the equation to solve is

$$(\frac{1}{\gamma}\mathrm{Id} + W)\boldsymbol{\alpha} = \boldsymbol{\beta}$$

References

Alvarez, L., Weickert, J., and Sánchez, J. (2000). Reliable Estimation of Dense Optical Flow Fields with Large Displacements. *Int. J. of Comp. Vision*, 39(1):41 – 56.

Amini, A. A., Chen, Y., and Abendschein, D. (1999). Comparison of Landmark-Based and Curve-Based Thin-Plate Warps for Analysis of Left-Ventricular Motion from Tagged MRI. In *Proc. of MICCAI'99*, volume 1679 of *LNCS*, pages 498 – 507, Cambridge, UK. Springer.

Brady, M. and Horn, B. K. P. (1983). Rotationally Symmetric Operators for Surface Interpolation. *Comp. Vision, Graphics, and Image Processing*, 22:70 – 94.

Cachier, P. and Ayache, N. (2001). Regularization in Image Non-Rigid Registration: I. Trade-Off between Smoothness and Similarity. Technical Report RR-4188, INRIA. `http://www.inria.fr/rrrt/`.

Cachier, P., Mangin, J.-F., Pennec, X., Rivière, D., Papadopoulos-Orfanos, D., Régis, J., and Ayache, N. (2001). Multisubject Non-Rigid Registration of Brain MRI using Intensity and Geometric Features. In *Proc. of MICCAI'01*. in press.

Cachier, P. and Pennec, X. (2000). 3D Non-Rigid Registration by Gradient Descent on a Gaussian-Windowed Similarity Measure using Convolutions. In *Proc. of MMBIA'00*, pages 182 – 189, Hilton Head Island, USA. `http://www-sop.inria.fr/epidaure/personnel/Pascal.Cachier/publi.html`.

Collignon, A., Maes, F., Delaere, D., Vandermeulen, D., Suetens, P., and Marchal, G. (1995). *Information Processing in Medical Imaging*, chapter Automated Multi-Modality Image Registration based on Information Theory, pages 263 – 274. Kluwer Academic Publishers.

Davis, M. H., Khotanzad, A., Flamig, D. P., and Harms, S. E. (1997). A Physics-Based Coordinate Transformation for 3D Image Matching. *IEEE Trans. on Medical Imaging*, 16(3):317 – 328.

Deriche, R. (1993). Recursively Implementing the Gaussian and its Derivatives. Technical Report RR-1893, INRIA.

Duchon, J. (1976). Interpolation des fonctions de deux variables suivant le principe de la flexion des plaques minces. *RAIRO Analyse Numérique*, 10(12):5 – 12.

Ferrant, M., Warfield, S. K., Guttmann, C. R. G., Mulkern, R. V., Jolesz, F. A., and Kikinis, R. (1999). 3D Image Matching using a Finite Element Based Elastic Deformation Model. In *Proc. of MICCAI'99*, volume 1679 of *LNCS*, pages 202 – 209, Cambridge, UK. Springer.

Gee, J. C., Le Briquer, L., Barillot, C., Haynor, D. R., and Bajcsy, R. (1995). Bayesian Approach to the Brain Image Matching Problem. In *SPIE Medical Imaging*.

Hellier, P., Barillot, C., Mémin, E., and Pérez, P. (1999). Medical Image Registration with Robust Multigrid Techniques. In *Proc. of MICCAI'99*, volume 1679 of *LNCS*, pages 680 – 687, Cambridge, UK. Springer.

Hermosillo, G., Chefd'Hotel, C., and Faugeras, O. (2001). A Variational Approach to Multi-Modal Image Matching. Technical Report RR-4117, INRIA.

Holden, M., Hill, D. L. G., Denton, E. R. E., Jarosz, J. M., Cox, T. C. S., Rohlfing, T., Goodey, J., and Hawkes, D. J. (2000). Voxel Similarity Measures for 3-D Serial MR Brain Image Registration. *IEEE Trans. on Medical Imaging*, 19(2):94 – 102.

Jeffreys, H. (1973). On Isotropic Tensors. *Proc. of Cambridge Phil. Soc.*, 73:173 – 176.

Kannappan, P. and Sahoo, P. K. (1992). Rotation Invariant Separable Functions are Gaussian. *SIAM J. on Mathematical Analysis*, 23(5):1342 – 1351.

Lakes, R. (1987). Foam Structures with a negative Poisson's ratio. *Science*, 235(4792):1038 – 1040.

Miller, M. I., Christensen, G. E., Amit, Y., and Grenander, U. (1993). Mathematical Textbook of Deformable Neuroanatomies. *Proc. of the National Academy of Science*, 90(24):11944–11948.

Nielsen, M., Florack, L., and Deriche, R. (1994). Regularization and Scale Space. Technical Report RR-2352, INRIA.

Nikou, C., Heitz, F., and Armspach, J.-P. (1999). Robust voxel similarity metrics for the registration of dissimilar single and multimodal images. *Pattern Recognition*, 32(8):1351 – 1368.

Rey, D., Subsol, G., Delingette, H., and Ayache, N. (1999). Automatic Detection and Segmentation of Evolving Processes in 3D Medical Images: Application to Multiple Sclerosis. In *Proc. of IPMI'99*, volume 1613 of *LNCS*, pages 154–167, Visegrád, Hungary.

Roche, A., Malandain, G., Pennec, X., and Ayache, N. (1998). Multimodal Image Registration by Maximization of the Correlation Ratio. Technical Report RR-3378, INRIA.

Rohr, K., Fornefett, M., and Stiehl, H. S. (1999). Approximating Thin-Plate Splines for Elastic Registration: Integration of Landmark Errors and Orientation Attributes. In *Proc. of IPMI'99*, volume 1613 of *LNCS*, pages 252 – 265, Visegrád, Hungary. Springer.

Rueckert, D., Sonoda, L., Hayes, C., Hill, D., Leach, M., and Hawkes, D. (1999). Nonrigid registration using free-form deformations: application to breast MR images. *IEEE Trans. on Medical Imaging*, 18(8):712 – 721.

Smith, G. F. (1968). On Isotropic Tensors and Rotation Tensors of Dimension m and Order n. *Tensor, N. S.*, 19:79 – 88.

Studholme, C., Hill, D. L. G., and Hawkes, D. J. (1995). *Information Processing in Medical Imaging*, chapter Multiresolution Voxel Similarity Measures for MR-PET Registration, pages 287–298. Kluwer Academic Publishers.

Studholme, C., Hill, D. L. G., and Hawkes, D. J. (1999). An Overlap Invariant Entropy Measure of 3D Medical Image Alignment. *Pattern Recognition*, 32(1):71 – 86. `http://www.elsevier.nl/inca/publications/store/3/2/8`.

Terzopoulos, D. (1986). Regularization of Inverse Visual Problems Involving Discontinuities. *IEEE Trans. on Pattern Analysis and Machine Intelligence*, 8(4).

Tsai, A., Yezzi, A., and Willsky, A. S. (2000). A Curve Evolution Approach to Medical Image Magnification via the Mumford-Shah Functional. In *Proc. of MICCAI'00*, number 1935 in LNCS, pages 246 – 255, Pittsburgh, USA. Springer.

Weese, J., Rösch, P., Netsch, T., Blaffert, T., and Quist, M. (1999). Gray-Value Based Registration of CT and MR Images by Maximization of Local Correlation. In *Proc. of MICCAI'99*, volume 1679 of *LNCS*, pages 656 – 663, Cambridge, UK. Springer.

Wells, W. M., Viola, P., Atsumi, H., Nakajima, S., and Kikinis, R. (1996). Multi-Modal Volume Registration by Maximization of Mutal Information. *Medical Image Analysis*, 1(1):35–51.

Weyl, H. (1966). *The Classical Groups: their invariants and representations.* Princeton University Press.

Unité de recherche INRIA Sophia Antipolis
2004, route des Lucioles - BP 93 - 06902 Sophia Antipolis Cedex (France)

Unité de recherche INRIA Lorraine : LORIA, Technopôle de Nancy-Brabois - Campus scientifique
615, rue du Jardin Botanique - BP 101 - 54602 Villers-lès-Nancy Cedex (France)
Unité de recherche INRIA Rennes : IRISA, Campus universitaire de Beaulieu - 35042 Rennes Cedex (France)
Unité de recherche INRIA Rhône-Alpes : 655, avenue de l'Europe - 38330 Montbonnot-St-Martin (France)
Unité de recherche INRIA Rocquencourt : Domaine de Voluceau - Rocquencourt - BP 105 - 78153 Le Chesnay Cedex (France)

Éditeur
INRIA - Domaine de Voluceau - Rocquencourt, BP 105 - 78153 Le Chesnay Cedex (France)
http://www.inria.fr
ISSN 0249-6399